JOURNAL OF MATERIALS SCIENCE 29 (1994) 3955–3963

Photo-oxidation of polystyrene under load

B. O'DONNELL, J. R. WHITE
Materials Division, Department of Mechanical, Materials and Manufacturing Engineering, University of Newcastle upon Tyne, Newcastle upon Tyne, NE1 7RU, UK

The effect of a tensile stress on the rate of photo-oxidation of polystyrene was investigated. Molecular-weight measurements showed that tensile stress accelerates molecular scission in injection-moulded bars exposed to ultraviolet irradiation. Changes in the residual-stress distribution were observed during the exposure but they were not sufficient to reverse the sense of the residual stresses, and the residual stress near the surface remained compressive. Depth profiling indicated that the degradation process was oxygen-diffusion limited and an approximate analysis of the kinetics gave an activation energy for degradation of 4.2 kJ m^{-2}, which is also consistent with a diffusion process.

1. Introduction

The main objective of the study reported here was to conduct experiments to confirm that stress accelerates the photo-oxidative degradation of polymers. The idea that stress can assist chemical reactions is well-established and *mechanico-oxidative degradation* in rubbers has been long recognized. The book by Davis and Sims [1] suggests that polymers are likely to fail more rapidly if weathered under load, but it does not refer to any quantitative studies of this effect. Significant research has been conducted into the acceleration of the thermo-oxidative degradation of thermoplastics. Much of this work was conducted in the former Soviet Union and is reviewed in a monograph [2]; further discussion is included in a recent review [3]. Much of the data obtained on stress-assisted thermo-oxidation of polymers can be fitted to the rate law that is usually attributed to Zhurkov [4, 5]

$$r = A\exp[-(\Delta G - B\sigma)/RT] \qquad (1)$$

where r is the rate of a process that has an activation energy, ΔG, σ is the stress, R is the gas constant and T is the absolute temperature, and A and B are constants.

Photo-oxidation involving the ultraviolet (u.v.) component of solar radiation is generally accepted as the principal cause of the outdoor degradation of polymers, and the studies described here were designed to investigate whether stress-assisted photo-oxidation could be described in a similar manner. An important feature of this work was the periodic measurement of the residual-stress distribution in test pieces, so that the influence of residual stresses (rather than the applied stresses) could be assessed.

2. Experimental procedure

2.1. Specimen preparation

The material chosen for the investigation was polystyrene (PS) because of the considerable knowledge and experience with this material derived from several studies of residual stress, natural weathering and fracture behaviour [6–12]. The grade used was BP HH101, provided by BP Chemicals and described as containing no u.v. stabilizer. Samples were made in the form of injection-moulded bars measuring approximately $190 \times 12.7 \times 3.2$ mm^3 using a tool with an end-gated cavity. Samples were moulded in large batches; several mouldings were rejected at the beginning of each run to ensure the machine had reached equilibrium. The injection pressure was 175 MPa, and the temperatures were: barrel 150/200 °C, nozzle 170 °C and mould 40 °C. The samples were stored in the dark in a room held at 30 ± 0.5 °C.

2.2. Illumination arrangement

Fluorescent tubes of type UVA-340 (Q-Panel Company) were used as the u.v. radiation source. The tubes used were chosen because their output in the u.v. matches the spectrum of solar radiation at the Earth's surface fairly closely. The supplier's own data showed that the match was extremely close in the wavelength range below 360 nm down to the cut-off at approximately 295 nm [13]. This has been confirmed by measurements of the spectral output of the UVA-340 tubes made using a Bentham Instruments spectroradiometer based on a double-grating monochromator (Fig. 1).

The tubes were approximately 1.2 m long with a fairly uniform output over the central metre. They were used in pairs, and the tube axes were set approximately 57 mm apart in the uniaxial creep rigs (see below). Measurements have shown that the illumination falling onto a flat test piece with its axis perpendicular to the tube axes is fairly uniform over the gauge length. The separation between the test piece surface and the plane containing the tube axes was 44 mm, and this gave an intensity of 4 W m^{-2} in the wavelength range 295–320 nm, that is, the total radiation below a wavelength of 320 nm. This corresponds closely to the midsummer intensity at noon in Jeddah, Saudi Arabia, which has one of the most

0022-2461 © 1994 Chapman & Hall

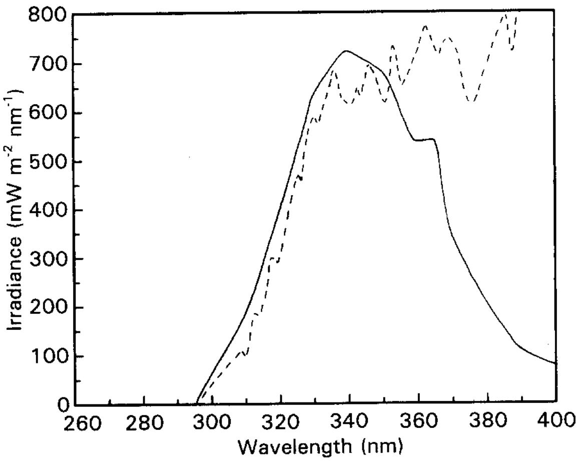

Figure 1 (——) The spectral output of UVA-340 fluorescent tubes: measured with the spectroradiometer, and (---) the solar spectrum.

severe climates in which polymer weathering trials have been conducted [10, 12, 14–17]. The daily dose for samples exposed in the laboratory under these conditions was therefore 96 W h m^{-2} which should be compared to the daily u.v. dose within this wavelength range in Jeddah in midsummer of 20 W h m^{-2}.

The illumination provided by the tubes was checked regularly using a Bentham Instruments spectroradiometer. The calibration of the instrument was checked every 3–4 months using a standard lamp delivering wavelengths in the range 250–3000 nm (Bentham Instruments model CL2).

The illumination level diminished as the u.v. penetrated deeper into the bar and it was necessary to know the absorption coefficient in order that the intensity could be determined at all depths. The method used was to measure the transmission through a bar and then to mill away a layer 0.1–0.2 mm thick, to polish the milled surface, and then to measure the transmission again. This was repeated until only 0.1–0.2 mm remained. The expected relationship between the intensity, $I(z)$, and the depth, z, within the bar is

$$I(z) = I(0)\exp(-\mu z) \qquad (2)$$

where $I(0)$ is the intensity at the entry face and μ is the absorption coefficient. Note that $I(0)$ is not the unimpeded intensity, I_0, measured in the absence of a bar, but it is the unimpeded intensity minus the reflected component at the entrance face. From Equation 2,

$$\ln I(z) = \ln I(0) - \mu z \qquad (3)$$

The measured intensity, I, escaping from the exit face is less than $I(z)$ because of internal reflection.
Thus

$$I(0) = I_0(1 - r^2)$$

and

$$I = I(z)(1 - r^2)$$

where r is the reflectivity.
Hence

$$\ln[I/(1 - r^2)] = \ln[I_0(1 - r^2)] - \mu z$$

or

$$\ln I = \ln[I_0(1 - r^2)^2] - \mu z \qquad (4)$$

so that a plot of $\ln I$ versus z should give a straight line of gradient μ. The intercept, $\ln I_i$, on the $\ln I$ axis can be compared with the measurement of the unimpeded intensity, I_0, to give the reflectivity, r, of the polymer using the following equation.

$$(1 - r^2)^2 = I_i/I_0 \qquad (5)$$

2.3. Loading arrangement, uniaxial creep

A simple uniaxial creep rig was designed in which a dead weight load was applied to the test piece via a lever arm. The rigs had a load cell attached co-axially to the test piece. The rigs were arranged side by side and three or four were illuminated by the same pair of tubes. Unloaded control samples were placed alongside the test pieces under load.

Some preliminary tests were carried out to find a suitable load range. It was considered necessary to use loads that would not cause failure during an extended period in the absence of u.v. Bars loaded at 10 MN m^{-2} under normal laboratory lighting conditions (for which the intensity for wavelengths below 320 nm was less than 0.005 W m^{-2}) formed fine crazes within 4 weeks but they had not broken when the test was terminated after 8 weeks. U.V. exposures were consequently made with creep loads set to give stresses of 7, 8, 9 and 10 MN m^{-2}.

2.4. Temperature control

All the artificial weathering was conducted at a constant temperature. The majority of the rigs were placed in a constant-temperature room set at 30 °C; the temperature fluctuated by less than ± 1 ° and the temperature was between 29.9 °C and 30.5 °C. Some rigs were located in a different laboratory and they were fitted with specimen enclosures which are used for conditioning at other temperatures. The enclosure had a U-shaped duct attached to it that contained a heater coil and an in-line low-power fan that ran at a constant speed. The heater current was regulated by a temperature controller that was connected to a temperature sensor (usually a resistance thermometer) placed alongside the test piece. Thus, in addition to the tests carried out at 30 °C, a smaller programme was conducted at temperatures of 50 and 73 ° C, using a stress of 10 MN m^{-2} and unstressed control samples, at an exposure intensity of 4 W m^{-2}.

There was no humidity control in the constant-temperature room. The relative humidity was measured regularly and it was found to vary between 20% and 30%.

2.5. Residual-stress measurement

All of the stress levels quoted above are applied stresses. Injection mouldings contain residual stresses. The residual stress at a given location should be added to the applied stress at that point to give the total stress. The residual stresses change during an extended period of observation as the result of relaxation processes, and the change in the residual stress may be influenced by the thermo-mechanical and/or the chemical conditions that prevail. Thus, part of the experimental programme was directed at measuring residual-stress levels after selected representative exposure periods.

Residual stresses were measured using the layer-removal procedure [8, 18, 19]. In this method thin layers (ca. 0.1 mm thick) were removed from the surface of the bar using high-speed milling with a single-point cutter and a fly-cutting action. After each layer removal, the bar was released from the milling bed and its curvature was measured. If residual stresses were present the removal of material from one side altered their distribution, and from a plot of curvature versus the depth removed the original stress distribution could be computed [8, 18, 19]. The analysis presented by Treuting and Read [19] assumed that the Young's modulus is uniform throughout, a condition from which injection mouldings often depart significantly, and which is most unlikely to be shown by bars degraded preferentially from the surface. Nevertheless, the simple application of the Treuting-Read analysis usually provides results that are not seriously in error [20, 21] and this analysis was used here.

Earlier investigations studied the effect of weathering on residual-stress distributions in injection mouldings [10, 12, 16, 17]. Although it is of interest to examine how residual stresses change during photo-oxidation in the laboratory, the emphasis in our experiments was different and the residual-stress distribution was required so that the stress could be estimated at each location within the bar. The stress at a particular location is the algebraic sum of the applied stress and the residual stress. It is admitted that the local applied stress will not equal the average applied stress calculated from the applied load when the sample possesses a non-uniform Young's modulus, but this was ignored in our initial analyses.

Samples were periodically removed for residual-stress analysis during the exposure runs. Machined chippings were saved for molecular-weight analysis by gel-permeation chromatography (GPC) (see Section 2.6).

2.6. Molecular-weight measurement

Samples for molecular-weight analysis were generally prepared by milling material from injection-moulded bars using a single-point cutter with a fly-cutting action. The machine swarf or chips were collected for analysis by GPC. Before standardizing this procedure, a preliminary investigation was made to check whether the sample-preparation procedure caused any molecular damage. Comparisons were made of results obtained from a sample prepared in this manner from the surface of an unexposed bar and of material from the opposite face in the form of a thin tape which was the remainder after a series of layer removals. The results were indistinguishable, and it was deduced that the machining process did not cause any significant molecular degradation [22]. This meant that samples could be prepared in this way for all chosen depths from a single bar. Approximately 0.2 mm was removed from the bar surface each time. Material for molecular-weight measurement was taken from the central 70 mm of the gauge length. This provided a sample from each depth of ca. 0.2 g, which was sufficient to make two GPC runs; a second run was made in most cases. Comparison with results obtained with virgin material showed that very little degradation took place during injection moulding [22].

The molecular-weight analysis of the samples was carried out by GPC at Rapra Technology Ltd. using the standard systems and procedures of the Polymer Supply and Characterisation Centre. The columns used were Polymer Laboratories PL gel 2 × mixed gel-B, with a column length of 300 mm and a particle size of 10 μm. The solvent used was tetrahydrofuran and the solution concentration was 2.0 $\mathrm{kg\,dm^{-3}}$. The injection volume was 0.2 ml and the flow rate was 1.0 $\mathrm{ml\,min^{-1}}$; the temperature was less than 30 °C.

The system was calibrated with narrow-molecular-weight-distribution polystyrene calibrants (Polymer Laboratories Ltd) and the data were processed using GPC-PRO software (Viscotek Corporation).

Sample solutions of polystyrene were prepared the day before the chromatography. A small amount of 1,2-dichlorobenzene was added as an internal marker and the solutions were filtered through a 0.2 μm polyamide membrane.

The results were presented as number-averaged molecular weight, M_n, weight-averaged molecular weight, M_w, and as continuous-size-distribution plots versus molecular weight. A reference sample cut from a virgin pellet of the polymer under examination was run at the beginning of each batch of GPC runs.

The GPC method is not particularly reliable at the low-molecular-weight end of the size spectrum. The absolute values are likely to be in doubt, and even data for comparison of samples of a similar type must be obtained using strictly controlled procedures. Further discussion of the sources of error and the methods used to minimize inaccuracies is given elsewhere [22].

2.7. Mechanical testing

The samples were subjected to a tensile test after chosen periods of conditioning. Tests were conducted at a 20 $\mathrm{mm\,min^{-1}}$ crosshead speed. The samples were tested to fracture, and the fracture surfaces were retained for microscopical examination.

2.8. Surface morphology and fractography

Some fracture surfaces were examined in a light optical microscope, but most of the fractographic studies were made by scanning electron microscopy (SEM). Samples for examination by SEM were cut away about 5–10 mm below the fracture surface, then mounted on a SEM stub and gold-coated to minimize problems with radiation damage and charging [23]. The original surfaces of the moulding were examined in addition to the fracture surface, especially near the intersection with the fracture surface.

3. Results
3.1. General observations during artificial weathering

Under the u.v. irradiation used in this study, the polystyrene noticeably yellowed within 2 weeks at 30 °C, both in stressed and unstressed exposures. Yellowing developed more rapidly at the higher temperatures.

During creep loading under u.v. radiation at 30 °C, the bars quickly developed very fine crazes in the corners, first near the exposed surface and then near the back surface. A few crazes developed near the centre of both faces after prolonged exposure, but internal crazes were rarely found. No crazes were formed in the unstressed samples, but subsequent tensile testing and fractography confirmed that degradation had taken place during the u.v. exposure. At 50 and 73 °C the same sequence of craze development occurred but over a much shorter timespan. At longer exposures at the higher temperatures, irregular crazing appeared in the centre of both surfaces; this was more extensive than at 30 °C. No visible sign of crazing occurred in the unstressed samples even after 8 weeks at 73 °C and 4 $\mathrm{W m^{-2}}$.

3.2. Absorption-coefficient measurements

Fig. 2 shows the fraction of the incident u.v. radiation in the range below 320 nm that penetrated different thicknesses of samples prepared from polystyrene-moulded bars. The data in Fig. 2 are presented as $\log I$(= intensity), versus z (= depth) plots in Fig. 3. It is evident that, for a particular polymer, all of the data points with the exception of the point at zero depth are on a straight line. The measurement plotted at zero depth from the exposed surface in Fig. 2 is the incident radiation. A proportion of this is reflected, and there is a step change in intensity on moving an infinitesimal distance into the bar. The value just inside the surface is given by extrapolating the straight line back to meet the axis at zero depth. The reflectivity, r, of the material can be calculated from the intercept using Equation 5. The gradient of the $\log I$ versus z plot gives the absorption coefficient, μ. The values found using this analysis were

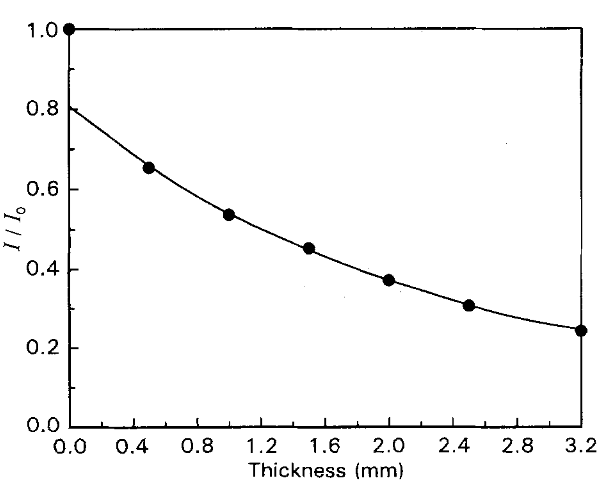

Figure 2 The normalized u.v. intensity versus the depth of penetration integrated over wavelengths in the range 295–320 nm (using UVA-340 tubes as the source).

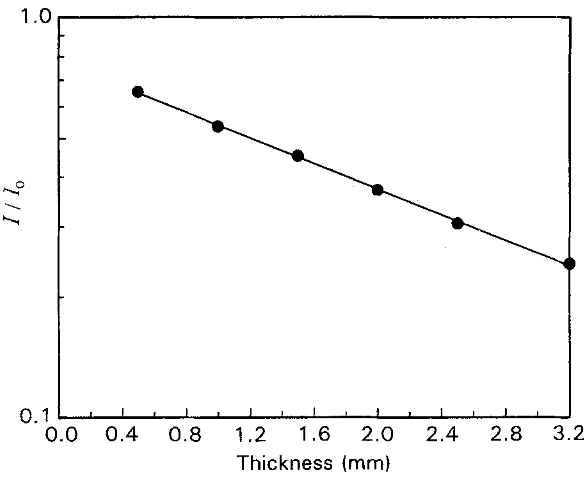

Figure 3 A plot of $\log(I/I_0)$ versus depth for polystyrene using the data plotted in Fig. 2.

Reflectivity	r	=	0.34
Absorption coefficient	μ	=	370 $\mathrm{m^{-1}}$

3.3. Molecular-weight measurements
3.3.1. Samples conditioned at 30 °C

Fig. 4 shows typical molecular-weight distributions for virgin polystyrene and for two degraded samples. The degraded samples were removed from the surfaces (~ 0.3 mm) of bars that were u.v. irradiated for 6 weeks, one in the unstressed state and the other with an applied stress of 10 $\mathrm{MN m^{-2}}$. Degradation is shown to have caused a shift to lower molecular weights. The shift observed with the sample from the stressed bar is greater than that with the unstressed bar. Of particular interest is the low-molecular-weight end because the presence of this fraction will be particularly detrimental to the properties of the material. This part of the GPC size spectrum is most prone to inaccuracies and careful assessment of the results must be made [22]. M_n will be much more sensitive than M_w to errors in the measurements of concentration of the low-molecular-weight species. It was found that scatter in the M_n-values from the control samples was greater than that in the M_w-values and this can probably be attributed to this increased sensitivity. The scatter in M_n in polystyrene was acceptably small when compared to the magnitude of the changes in values caused by photo-degradation. Fig. 4 also shows the size distribution measured for a sample removed from the surface (0.3 mm) of an as-moulded bar. The difference between this distribution and that obtained with the reference sample is negligible in comparison with that obtained with the exposed samples.

Fig. 5 shows plots of M_n versus depth for an as-moulded injection-moulded bar and for similar bars

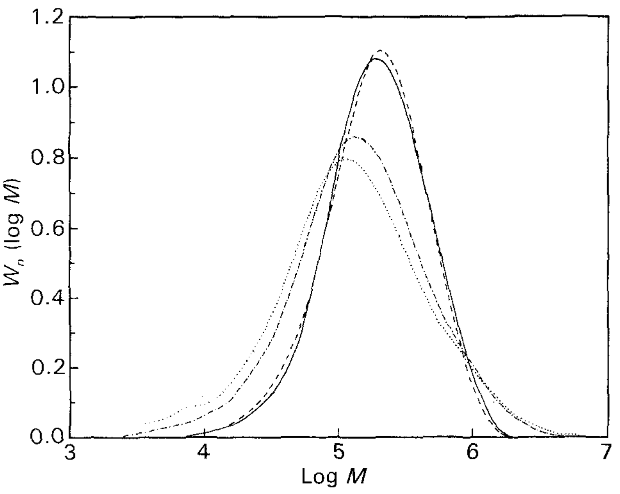

Figure 4 Molecular-weight distributions for polystyrene. (——) Virgin sample, (– – –) from the surface of an as-moulded bar, (·——·) from the exposed surface of a bar irradiated with u.v. for 6 weeks in the unstrained state, (· · ·) from the exposed surface of a bar irradiated with u.v. for 6 weeks at an applied stress of 10 MN m^{-2}. The exposures were conducted at 30 °C.

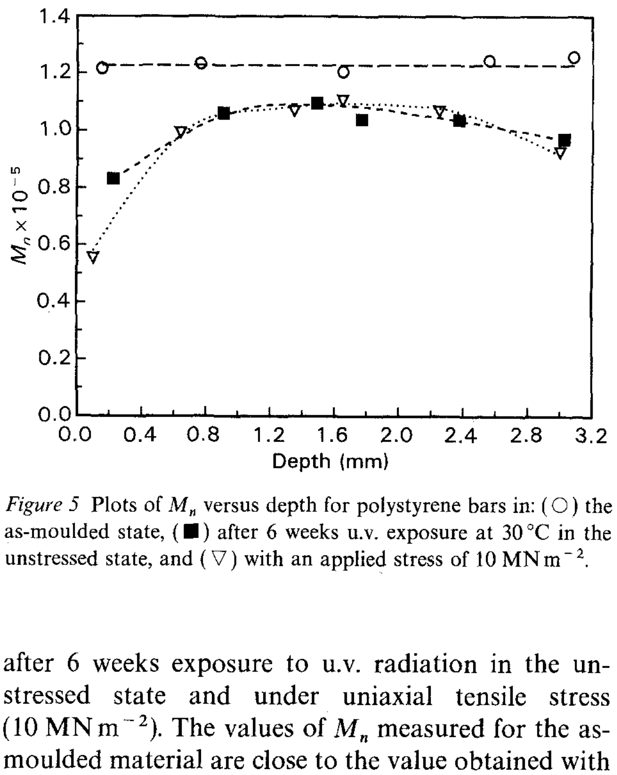

Figure 5 Plots of M_n versus depth for polystyrene bars in: (○) the as-moulded state, (■) after 6 weeks u.v. exposure at 30 °C in the unstressed state, and (▽) with an applied stress of 10 MN m^{-2}.

after 6 weeks exposure to u.v. radiation in the unstressed state and under uniaxial tensile stress (10 MN m^{-2}). The values of M_n measured for the as-moulded material are close to the value obtained with the virgin material (1.21 × 10^5) and it can be deduced that little or no molecular-weight degradation occurred during moulding. There is no evidence for depth-dependent differences in molecular weight in the as-moulded material; this indicates not only that degradation is not significant but also that there is no significant molecular-size segregation caused by flow during moulding. It should be noted that the sample taken from one side of the as-moulded bar was in the form of machine chippings and that taken from the other side in the form of a tape-like remainder. The agreement in the molecular-weight measurements from both samples is further evidence that the milling operation causes minimal molecular damage.

Significant molecular-weight degradation was caused by the u.v. treatment. The effect is greatest near the exposed surface. Degradation near the centre of the bar was small, but significant degradation was present near the surface that faced away from the u.v. source. It can be deduced that oxygen depletion in the centre inhibited reaction. Near the surfaces, the molecular weight in the stressed sample was lower than that in the unstressed sample, indicating that stress accelerates degradation; the effect was particularly pronounced near the exposed surface. Degradation in samples exposed for 2 weeks and for 4 weeks, was less advanced but they already showed the early stages of the development of depth and stress dependence.

3.3.2. Depth dependence and the effect of stress

To further investigate the depth dependence of degradation, the data were plotted as the molecular weight versus the total accumulated the dose, that is, the product of the dose rate and the exposure time. In this way data representing material exposed for different times and at different depths can be included on the same plot (recall that the intensity is known as a function of depth). The molecular weight at a particular depth was read from continuous plots such as that shown in Fig. 5. The data points in Fig. 5 are positioned at the midpoint of the layer from which the sample was taken. For example, if the first layer machined away was 0.3 mm thick, the corresponding value of M_n was plotted at 0.15 mm from the surface. Data for material located at the front and back surfaces of bars exposed for different times were obtained by extrapolation and are shown in Fig. 6. The data points representing a particular combination of depth and applied stress lie on approximately straight lines (see Appendix 1). The lines representing stressed samples are steeper than the corresponding lines for unstressed samples, confirming that stress accelerates molecular degradation.

An unexpected result was that the lines in Fig. 6 representing samples taken from the back face were steeper than those for samples from the exposed surface. This is presumably the consequence of oxygen starvation near the exposed surface, where the reaction is too fast for replenishment by diffusion. The measurements made at intermediate depths were consistent with this hypothesis. For example, results for depths 0.4 mm from the front and back faces are given in Fig. 7 and they show that the lines for the material located 0.4 mm from the exposed face are less steep than those for the material located at the exposed face (Fig. 6) and similarly that the gradients for the material 0.4 mm from the unexposed face are less than the corresponding values for the material at this surface. Oxygen starvation will naturally increase as the distance from the surface increases. The lines plotted in Fig. 7 for the bar irradiated under stress are steeper than those for the unstressed bar, confirming that stress has accelerated degradation. The gradients of plots made for material taken at still greater distances from the surfaces are still less steep and the effect of stress is likewise confirmed. It is evident that

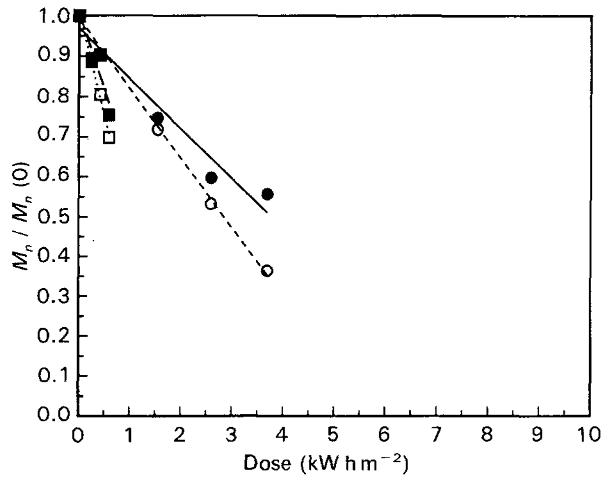

Figure 6 Plots of the ratio $M_n/M_n(0)$ for various u.v. doses at (●, ○) the exposed surface (0 mm) and (■, □) the unexposed surface (3.2 mm) of polystyrene bars irradiated at 30 °C (●, ■) unstressed and (○, □) with an applied stress of $10\ \mathrm{MN\,m^{-2}}$. ($M_n(0)$ is the value of M_n for a virgin sample.)

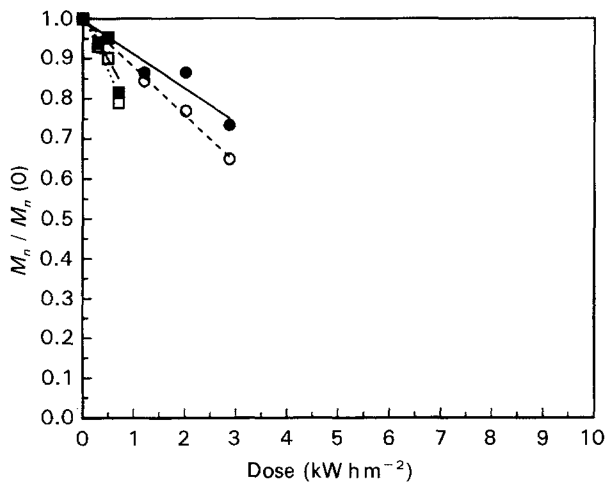

Figure 7 Plots of the ratio $M_n/M_n(0)$ for various u.v. doses 0.4 mm in from (●, ○) the exposed and (■, □) the unexposed surfaces of polystyrene bars irradiated at 30 °C (●, ■) unstressed and (○, □) with an applied stress of $10\ \mathrm{MN\,m^{-2}}$

the parameter, a, in Appendix 1 is a function of stress and of the depth within the moulding.

3.3.3. Samples conditioned at 50 and at 73 °C

Values for M_n obtained after 6 weeks of u.v. exposure at 50 °C for bars in both the unstressed state and with an applied tensile stress of $10\ \mathrm{MN\,m^{-2}}$ are plotted in Fig. 8. A line representing the data obtained for the as-moulded state is sketched in Fig. 8 (it was generated from the data points shown in Fig. 5). Degradation is more pronounced at the higher temperature and the stressed sample degraded more than the unstressed one. Degradation was even faster at 73 °C but the effect of stress appeared to be less influential than at lower temperatures (Fig. 9). Fig. 9 is compiled of data for a 3 week exposure because the samples did not survive 6 weeks of u.v. exposure under an applied stress of $10\ \mathrm{MN\,m^{-2}}$.

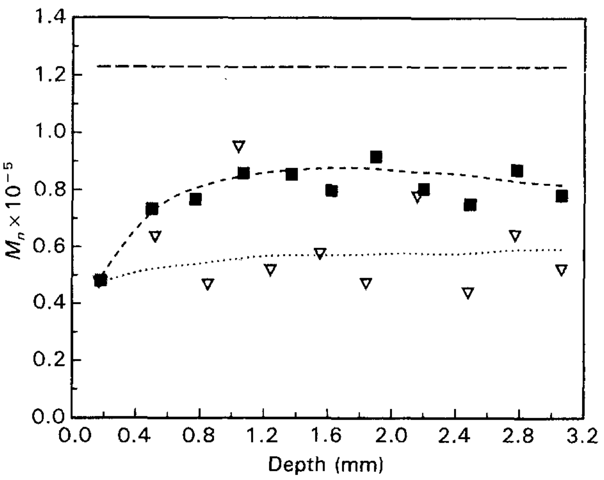

Figure 8 Plots of M_n versus depth for polystyrene bars in: (–––) the as-moulded state and (■) after 6 weeks of u.v. exposure at 50 °C in the unstressed state and (▽) with an applied stress of $10\ \mathrm{MN\,m^{-2}}$.

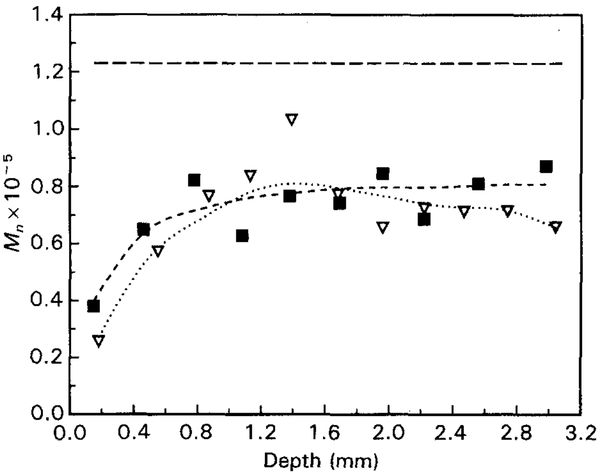

Figure 9 Plots of M_n versus depth for polystyrene bars after 3 weeks of u.v. exposure at 73 °C in: the (■) the unstressed state, and (▽) with an applied stress of $10\ \mathrm{MN\,m^{-2}}$.

3.3.4. Further analysis

The following expression is derived in Appendix 2 (it relates the activation parameters in Equation 1 with the initial number of molecules, $N(0)$, the initial number-averaged molecular weight, $M_n(0)$ and the number-averaged molecular weight at time t, $M_n(t)$.

$$\ln[N(0)/b] + \ln\{[M_n(0)/M_n(t) - 1]/t\} = -(\Delta G - B\sigma)/RT$$

Thus a plot of $\ln\{[M_n(0)/M_n(t) - 1]/t\}$ versus σ should give a straight line with a slope B/RT and an intercept $\{-\Delta G/RT - \ln[N(0)/b]\}$ where σ is taken to be the total stress (= applied stress + residual stress).

There was insufficient data to test the above analysis thoroughly, but the following illustration shows how it can be applied. We chose to select data from the exposed surfaces of bars tested in uniaxial creep conditions at three temperatures and for several residence times. The average residual stress within the layer at the surface sampled for the molecular-weight measurements was small (see below) and it was neglected in the approximate analysis presented here.

Fig. 10 shows a plot of $\ln\{[M_n(0)/M_n(t) - 1]/t\}$ versus σ for polystyrene samples taken from the exposed surfaces. Only two points were presented for tests conducted at 50 and at 73 °C and the required intercept was taken to be the value obtained directly at zero (applied) stress. The points obtained from tests at 30 °C lay on an approximately straight line for which the intercept coincided reasonably well with the direct zero-stress result. Fig. 11 shows a plot of these intercepts versus $1000/T$; the three points lie close to a straight line with a gradient of -503, giving a value for ΔG of 4.2 kJ mol^{-1}.

3.4. Residual-stress measurements

The as-moulded polystyrene contained weak residual stresses with a tensile maximum near to 1 MN m^{-2} near the centre and a maximum compressive stress of less than 3 MN m^{-2} just inside the surface. For the short exposure periods used, the stresses proceeded to decay slowly. The most important observation was that the stress sense remained the same for all the exposure times, with compressive stresses near the surface and tensile stresses in the interior. More discussion of this will be presented elsewhere [24].

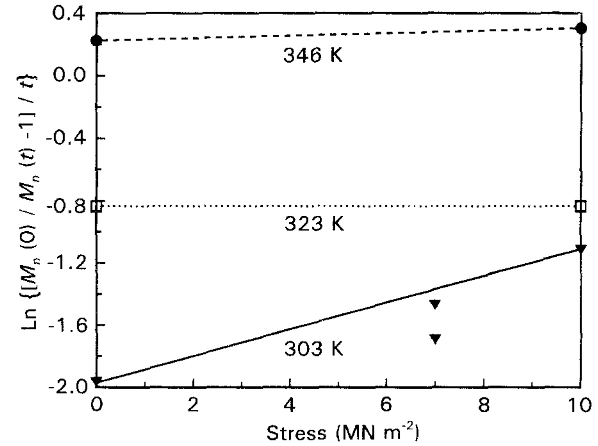

Figure 10 A plot of $\ln\{[M_n(0)/M_n(t) - 1]/t\}$ versus stress for polystyrene samples extracted from the exposed surfaces of bars tested for various times.

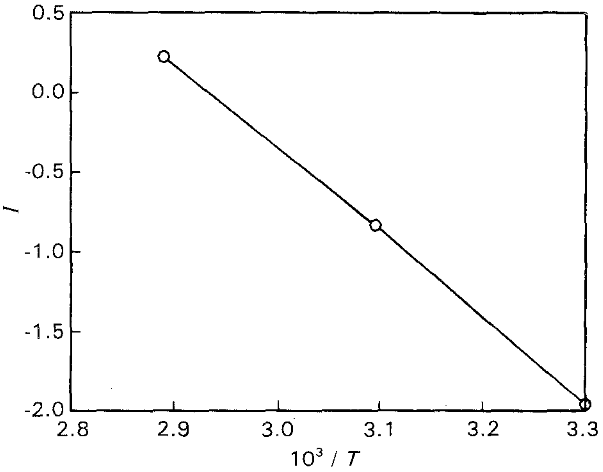

Figure 11 A plot of the intercepts, I, in Fig. 10 versus the reciprocal of the absolute temperature.

3.5. Mechanical-test results

The tensile strength of unexposed polystyrene was approximately 50 MN m^{-2} and it fell to about 26 MN m^{-2} after 4 weeks then it remained at roughly the same level (26 MN m^{-2}) after 6 weeks with both the stressed and the unstressed samples. The strength after 2 weeks was quite different for the unstressed samples (48 MN m^{-2}) and for the samples stressed at 10 MN m^{-2} in tension (30 MN m^{-2}).

3.6. Surface morphology and fractography

The fracture surfaces from samples which were tested in uniaxial tension without prior u.v. exposure showed features characteristic of polystyrene tested in this manner [25]. The unexposed bars failed from cracks nucleated in the interior at locations that were clearly visible on the fracture surface [24]. Many of the features were visible with a light optical microscope, but most observations were made by SEM because of the superior depth of field.

When exposed bars were subjected to a tensile test, the moulded surface that faced the u.v. source became crazed or cracked. Fig. 12 shows cracks in the surface of a polystyrene bar that was broken in tension after 6 weeks u.v. exposure onto the face shown. The surface cracks are reminiscent of those found after tensile-testing bars weathered outdoors in Jeddah with no applied strain [7, 12]. On inspection of the moulded faces, which were further from the u.v. source during exposure, it was found that there were no cracks present in bars which were given short exposures.

Polystyrene bars exposed for short periods in Jeddah or in the laboratory tended to fail by crack growth from an internal site [24]. Polystyrene bars exposed for intermediate times (for example, 6 weeks u.v. in the laboratory) tended to fail by crack growth from a corner site (Fig. 13); the corner in which fracture initiated was almost always on the exposed side of the bar. A similar cracking pattern was observed on the fracture surface of injection-moulded polystyrene under fatigue conditions [26].

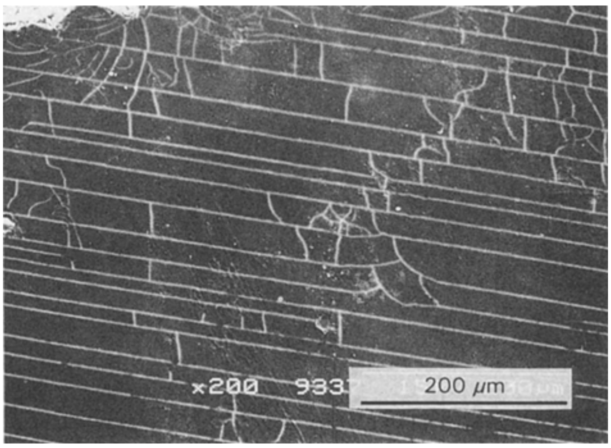

Figure 12 The moulded surface a polystyrene bar exposed to u.v. for 6 weeks and then broken in uniaxial tension (the side facing the u.v. source, at the fracture face).

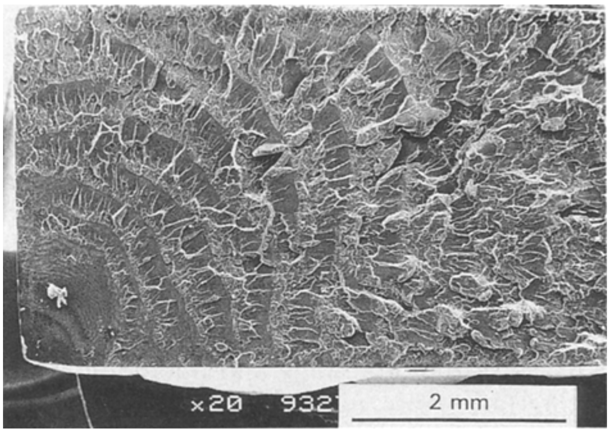

Figure 13 Polystyrene fracture surface for a sample in which failure nucleated at a corner.

4. Discussion and conclusions

The measurements of molecular weight on samples conditioned under various combinations of stress and u.v. illumination show conclusively that tensile stress accelerates molecular degradation in polystyrene. Accordingly, when polystyrene samples were tensile tested after these treatments, those samples which were conditioned under stress sometimes failed more readily than those which were conditioned in the unstressed state.

The residual stresses present in the bars, both in the as-moulded state and after various exposures, were generally fairly modest and they were much lower than the applied stresses in the trials performed under external loads. The residual stresses changed during u.v. exposure, but not as much as in some of the samples weathered outdoors [12, 16]. In particular, no development of tensile stresses at and near the exposed surface was found to occur. In earlier publications we suggested that this occurred during outdoor exposure of polystyrene, and some other polymers, as a consequence of the presence of temperature gradients rather than as the result of a photochemical reaction. The observations reported here are therefore consistent with this insofar as no tendency for the development of tensile residual stresses near the surface was found for samples conditioned under similar photochemical conditions and at a uniform temperature.

The variation in molecular degradation through the depth of bars irradiated in both the stressed and the unstressed state cannot be explained simply in terms of the difference in u.v. levels nor of the different levels of residual stress. The observations are consistent with the hypothesis that oxygen depletion is occurring. Comparison of degradation at the exposed and unexposed surfaces suggests that at high u.v. intensities the reaction rate is limited by oxygen concentration even in layers less than 100 μm thick. This is similar to the observations made on polyolefins [27]. The rather low activation energy of 4.2 kJ mol^{-1} that was derived from an approximate analysis of the kinetics of degradation is consistent with a diffusion-controlled process.

Degradation is particularly severe near the corners, and cracks tend to nucleate there after fairly short periods of exposure. This is probably because of the relatively easy access of oxygen allowed by the presence of two surfaces. It is evident that it is good practice to use rounded *external* corners and that in some circumstances this may be just as important as the well-established use of rounded internal corners (to minimize crack-promoting stress concentrations).

Appendix 1 Relationship between molecular weight and total accumulated dose

The value of the number-averaged molecular weight, $M_n(t)$, is given by

$$M_n(t) = M/N(t)$$

where M is the total mass of molecules and $N(t)$ is the number of molecules present. Therefore,

$$M_n(0) = M/N(0)$$

Each time there is a chain-scission event the number of molecules increases by one, and if the number of chain scissions is proportional to the dose, D, then

$$N(t) = N(0) + aD \qquad \text{(A1)}$$

where a is a constant provided that the reaction is insensitive to other factors. Hence

$$\begin{aligned} M_n(t)/M_n(0) &= N(0)/N(t) \\ &= \frac{N(0)}{N(0) + aD} \\ &= \{1 + [a/N(0)]D\}^{-1} \\ &= 1 - [a/N(0)]D \\ &\quad + [a/N(0)]^2 D^2 + \cdots \qquad \text{(A2)} \end{aligned}$$

Thus at low doses

$$M_n(t)/M_n(0) = 1 - [a/N(0)]D \qquad \text{(A3)}$$

Hence, for low doses, the ratio $M_n(t)/M_n(0)$ should fall linearly with D. This will be true as long as $[a/N(0)]D \gg [a/N(0)]^2 D^2$. Although this limits the validity of Equation A3 to values of $M_n(t)/M_n(0) > 0.9$, the departure from linearity will not be too rapid for lower values of $M_n(t)/M_n(0)$ (that is, for higher doses).

Appendix 2 The stress and temperature dependence of molecular-weight degradation

Starting from Equation 1, the rate of chain scission will be proportional to $\exp[-(\Delta G - B\sigma)/RT]$. Each scission event will cause the total number of molecules to increase by 1. Hence if the total number of scission events by time t is $n(t)$ and the number of molecules present at the beginning is $N(0)$, then the number of molecules after time t is

$$N(t) = N(0) + bt\exp[-(\Delta G + B\sigma)/RT]$$

where b is a constant. Thus the number-averaged molecular weight, M_n, can be written

$$M_n(t) = \frac{c}{N(t)} = \frac{c}{N(0) + bt\exp[-(\Delta G - B\sigma)/RT]}$$

The initial value of M_n is $M_n(0) = c/N(0)$. Hence

$$\frac{M_n(0)}{M_n(t)} = 1 + \frac{bt}{N(0)}\exp[-(\Delta G - B\sigma)/RT]$$

therefore,

$$\frac{N(0)}{bt}\left\{\frac{M_n(0)}{M_n(t)}\right\} = \exp[-(\Delta G - B\sigma)/RT]$$

Hence

$$\ln\left[\frac{N(0)}{b}\right] + \ln\left\{\left[\frac{M_n(0)}{M_n(t)} - 1\right]\Big/ t\right\} = \frac{-(\Delta G - B\sigma)}{RT}$$

Thus a plot of $\ln\{[M_n(0)/M_n(t) - 1]/t\}$ versus σ should give a straight line with a slope of B/RT and an intercept $\{-\Delta G/RT - \ln[N(0)/b]\}$ where σ is taken to be the total stress (= applied stress + residual stress). If these plots are obtained at different temperatures, the intercepts can be plotted against $1/T$ to give a straight line with a slope $-\Delta G/R$.

Acknowledgements

This project was supported by a SERC research grant. We are grateful to S. R. Holding of Rapra Technology Ltd for making the GPC molecular-weight measurements and for invaluable assistance in interpreting the results and assessing their reliability. The polystyrene was a generous gift from British Petroleum.

References

1. A. DAVIS and D. SIMS, "Weathering of polymers", (Applied Science, Barking, 1983).
2. A. POPOV, N. RAPOPORT and G. ZAIKOV, "Oxidation of stressed polymers" (Gordon and Breach, New York, 1991). (A translation of "Okislenie orientirovannykh i napryazheeykh polimerov" (Khimiya, Moscow, 1987)).
3. J. R. WHITE and A. TURNBULL, *J. Mater. Sci.* **29** (1994) 584.
4. H. H. KAUSCH, "Polymer fracture" (Springer-Verlag, New York, 1978).
5. S. N. ZHURKOV, V. A. ZAKREVSKYI, V. E. KORSUKOV and A. F. KUKSENKO, *J. Polym. Sci., Polym. Phys. Educ.* **10** (1972) 1509.
6. G. J. SANDILANDS and J. R. WHITE, *Polymer* **21** (1980) 338.
7. M. M. QAYYUM and J. R. WHITE, *ibid.* **23** (1982) 129.
8. B. HAWORTH, C. S. HINDLE, G. J. SANDILANDS and J. R. WHITE, *Plast. Rubb. Proc. Applics.* **2** (1982) 59.
9. M. THOMPSON and J. R. WHITE, *Polym. Engng. Sci.* **24** (1984) 227.
10. M. M. QAYYUM and J. R. WHITE, *J. Mater Sci.* **21** (1986) 2391.
11. A. V. IACOPI and J. R. WHITE, *J. Appl. Polym. Sci.* **33** (1987) 577.
12. M. M. QAYYUM and J. R. WHITE, *Arabian J. Sci. Engng.* **13** (1988) 545.
13. P. BRENNAN and C. FEDOR, 43rd Annual Conference of Composites Inst., SPI, Session 23-A, 1–5 February, 1988, Cincinnati (Society of Plastics Industry, New York, 1988) p. 1.
14. M. M. QAYYUM and A. DAVIS, *Polym. Degrad. Stab.* **6** (1984) 201.
15. M. M. QAYYUM and J. R. WHITE, *Polymer* **28** (1987) 469.
16. *Idem., J. Mater. Sci.* **20** (1985) 2557.
17. *Idem., Plast. Rubb. Proc. Applics.* **12** (1989) 171.
18. J. R. WHITE, *Polym. Testing* **4** (1984) 165.
19. R. G. TREUTING and W. T. READ Jr, *J. Appl. Phys.* **22** (1951) 130.
20. J. R. WHITE, *J. Mater. Sci.* **20** (1985) 2377.
21. M. W. A. PATERSON and J. R. WHITE, *ibid.* **24** (1989) 3521.
22. B. O'DONNELL, J. R. WHITE and S. R. HOLDING, *J. Appl. Polym. Sci.*, in press.
23. J. R. WHITE and E. L. THOMAS, *Rubb. Chem. Tech.* **57** (1984) 457.
24. LI TONG and J. R. WHITE, to be published.
25. P. BEAHAN, M. BEVIS and D. HULL, *Proc. Roy. Soc. Lond.* **A343** (1975) 525.
26. A. V. IACOPI and J. R. WHITE, *J. Appl. Polym. Sci.* **33** (1987) 577.
27. L. AUDOUIN, J. C. M. DEBRUIJN, V. LANGLOIS and J. VERDU, *J. Mater. Sci.* **29** (1994) 569.

Received 11 November 1993
and accepted 3 February 1994